



NIH PUBLIC ACCESS

Author Manuscript

Nat Neurosci. Author manuscript; available in PMC 2010 June 1.

Published in final edited form as:

Nat Neurosci. 2009 June ; 12(6): 777–783. doi:10.1038/nn.2327.

Ube3a is required for experience-dependent maturation of the neocortex

Koji Yashiro^{1,8}, Thorfinn T. Riday^{1,2}, Kathryn H. Condon⁶, Adam C. Roberts^{1,3,4}, Danilo R. Bernardo¹, Rohit Prakash¹, Richard J. Weinberg^{3,5}, Michael D. Ehlers^{6,7}, and Benjamin D. Philpot^{1,2,3,4}

¹Department of Cell and Molecular Physiology, University of North Carolina, Chapel Hill, NC 27599, USA

²Curriculum in Neurobiology, University of North Carolina, Chapel Hill, NC 27599, USA

³UNC Neuroscience Center, University of North Carolina, Chapel Hill, NC 27599, USA

⁴Neurodevelopmental Disorders Research Center, University of North Carolina, Chapel Hill, NC 27599, USA

⁵Department of Cell and Developmental Biology, University of North Carolina, Chapel Hill, NC 27599, USA

⁶Department of Neurobiology Duke University Medical Center, Durham, NC 27710, USA

⁷Howard Hughes Medical Institute, Duke University Medical Center, Durham, NC 27710, USA

⁸K.Y. present address: Urogenix Inc, Durham NC 27713, USA

Abstract

Experience-dependent maturation of neocortical circuits is required for normal sensory and cognitive abilities, which are distorted in neurodevelopmental disorders. We have tested whether experience-dependent neocortical modifications require Ube3a, an E3 ubiquitin ligase whose dysregulation has been implicated in autism and Angelman syndrome (AS). Using visual cortex as a model, we demonstrate that experience-dependent maturation of excitatory cortical circuits is severely impaired in AS mice deficient in Ube3a. This developmental defect is associated with profound impairments in neocortical plasticity. Remarkably, normal plasticity is preserved under conditions of sensory deprivation, but rapidly lost by sensory experiences. The loss of neocortical plasticity is reversible, as late-onset visual deprivation restores normal synaptic plasticity. Further, Ube3a-deficient mice lack ocular dominance plasticity *in vivo* when challenged with monocular deprivation. These results show that Ube3a is necessary to maintain plasticity during experience-dependent neocortical development, and suggest that loss of neocortical plasticity contributes to deficits associated with AS.

Co-Correspondence: Michael D. Ehlers, Howard Hughes Medical Institute, Duke University Medical Center, Box 3209, 317 Bryan Research Building, Research Dr., Durham, NC 27710, Tel: (919) 684-1828, Fax: (919) 668-0631, Email: ehlers@neuro.duke.edu; Benjamin D. Philpot, University of North Carolina, Campus Box 7545, 115 Mason Farm Road, Chapel Hill, NC, 27599-7545, Tel: (919) 966-0025, Fax: (919) 966-6927, Email: bphilpot@med.unc.edu.

Competing interests statement: The authors declare no competing financial interests.

Author contributions: K.Y., B.D.P., and M.D.E designed the study and wrote the manuscript. K.Y. conducted immunohistochemistry, Golgi impregnation, whole-cell patch-clamp, and field potential experiments. T.T.R. contributed to field potential studies and conducted visual evoked potential experiments. K.H.C. contributed to Golgi impregnation study and conducted immunoblot experiments. A.C.R. contributed to whole-cell patch-clamp and field potential studies. D.R.B. contributed to field potential studies. R.P. contributed to visual evoked potential experiments. R.J.W. directed the Golgi impregnation experiments and helped to prepare the manuscript. M.D.E. and B.D.P. supervised the study.

Introduction

Angelman syndrome (AS) is a severe hereditary mental retardation characterized by outwardly normal development during the first year of life with a profound absence of subsequent cognitive milestones such as speech, despite a normal life span^{1,2}. AS is caused by loss-of-function mutations or deletions in the maternally inherited allele of *UBE3A*³, a gene whose dysregulation is also implicated in autism⁴. *UBE3A* encodes a HECT domain ubiquitin E3 ligase which, in the brain, is expressed primarily from the maternal allele due to tissue-specific imprinting^{2,5,6}. The apparent lack of neurodegeneration² and the sharp postnatal onset of symptoms in AS has suggested a developmental defect in synaptic circuits⁷, whose origin is unknown. Interestingly, mice deficient in maternal Ube3a exhibit genetically-reversible impairments both in learning and hippocampal LTP^{2,8,9}, pointing to deficits in synaptic plasticity. Moreover, recent studies have demonstrated the involvement of the ubiquitin proteasome system in synaptic development and plasticity^{10,11}, raising the possibility that Ube3a-mediated protein degradation may be involved in these processes.

Despite a documented role of Ube3a in learning^{2,9}, it is not known how Ube3a affects the neocortex, a brain region that is heavily sculpted through experience-dependent development and whose disruption could explain most AS deficits. Combined with the early postnatal emergence of AS-related deficits and the clinical observations that AS patients present behaviors consistent with altered sensory processing^{12,13}, the learning deficits associated with AS led us to hypothesize that Ube3a regulates experience-dependent refinement of neuronal circuits dependent upon sensory input.

We used the visual cortex as a model system¹⁴⁻²⁰ to study the role of Ube3a in experience-dependent plasticity of the neocortex in a maternally-deficient AS mouse model (Ube3a^{m-/p+}). Our results demonstrate an unexpected role for Ube3a in maintaining synaptic plasticity in the face of sensory processing, and suggest a basis for the learning deficits associated with Angelman syndrome.

Results

Reduced maturation of neocortical synapses in AS mice

Although Ube3a^{m-/p+} mice exhibit extensive loss of Ube3a due to maternal imprinting in many areas of the brain including the cerebellum, hippocampus, and parts of the neocortex^{2,5,6,21}, it is unknown whether this also occurs within the visual cortex. Immunoblot analysis revealed that paternal deficiency in Ube3a (Ube3a^{m+/p-}) does not alter Ube3a protein levels in the hippocampus, cerebellum, and visual cortex (Fig. 1a). In contrast, Ube3a expression was drastically reduced in Ube3a^{m-/p+} mice compared to wild-type (WT) mice in all three brain regions. Consistent with previous observations^{3,22}, this attenuation was brain-specific, because Ube3a was highly expressed in the liver of both Ube3a^{m+/p-} and Ube3a^{m-/p+} mice (Fig. 1a). We verified maternal imprinting of Ube3a protein using immunohistochemistry. Ube3a immunostaining was prominent in the visual cortex of WT mice, but marginally detectable in Ube3a^{-/-} and Ube3a^{m-/p+} mice (Fig. 1b and Supplementary Fig. 1a). In WT mice, cells immunopositive for the neuronal marker NeuN²³ stained intensely for Ube3a (Fig. 1b). Immunoblot analysis of whole cortex homogenates (Supplementary Fig. 1b) and immunohistochemistry (data not shown) revealed that maternal imprinting is a general feature of neocortical Ube3a expression and is not unique to the visual cortex.

To determine the physiological consequence of Ube3a loss on neocortical development, we examined the developmental acquisition of spontaneous excitatory synaptic transmission by recording miniature excitatory postsynaptic currents (mEPSCs) in layer 2/3 pyramidal neurons

of visual cortex (see Supplementary Table 1 for intrinsic membrane properties of recorded neurons). Consistent with previous findings^{24,25}, mEPSC amplitudes decreased and frequency increased during development in WT mice (Fig. 1c-e). Just prior to eye opening (P10), mEPSC frequency and amplitude were indistinguishable between WT and Ube3a^{m-/p+} mice (Fig. 1c-e). Thereafter, mEPSC frequency failed to develop normally in Ube3a^{m-/p+} mice (Fig. 1c,e). Despite reductions in mEPSC frequency, signatures of postsynaptic neurotransmission appeared normal at extant synapses in Ube3a^{m-/p+} mice, because both mEPSC amplitude (Fig. 1d) and the ratio of AMPA to NMDA responses (Supplementary Fig. 2) were comparable between WT and Ube3a^{m-/p+} mice.

Experience-dependent maturation of synapses requires Ube3a

Because mEPSC deficits began to appear after eye opening and the onset of patterned vision (P11-12 in the mouse), we investigated the role of visual experience in regulating the development of spontaneous synaptic activity in Ube3a^{m-/p+} mice. Toward this end, we dark-reared (DR) animals from P10 until P25 to deprive them of visual experience after eye opening, and compared mEPSC frequency and amplitude in layer 2/3 pyramidal neurons to that of normally-reared (NR) mice (Fig. 2a). Although dark-rearing had no measurable effect on mEPSC amplitude in WT mice at P25 (Fig. 2b, c), sensory deprivation strongly attenuated the normal developmental increase in mEPSC frequency in WT mice (Fig. 2b, d). In contrast, dark-rearing affected neither mEPSC amplitude (Fig. 2b, c) nor frequency (Fig. 2b, d) in Ube3a^{m-/p+} mice. Consequently, mEPSC frequency in NR Ube3a^{m-/p+} mice was not significantly different from that of DR WT mice ($p = 0.79$) (Fig. 2d). These findings demonstrate that, although Ube3a is not necessary for the initial sensory-independent establishment of synaptic connectivity, it is selectively required for experience-dependent maturation of excitatory circuits.

The decrease in mEPSC frequency raised the possibility that layer 2/3 excitatory synapses are functionally lost in the absence of Ube3a. To examine this further, we used Golgi impregnation to test for experience-dependent differences in dendritic spines (Fig. 2e), the anatomical site where most excitatory synaptic connections are made²⁶. Although spine density of layer 2/3 visual cortical pyramidal neurons was comparable between DR WT and DR Ube3a^{m-/p+} mice (Fig. 2f), it was significantly lower in NR Ube3a^{m-/p+} mice compared to NR WT mice (Fig. 2f), consistent with previous observations in other neocortical regions of normally reared mice⁶. Together with the electrophysiological observations, these data demonstrate that Ube3a^{m-/p+} mice are defective in experience-dependent development of excitatory synaptic connections.

Synaptic plasticity is impaired in neocortex of AS mice

One possible explanation for the lack of experience-dependent synaptic development in Ube3a^{m-/p+} mice is defective activity-dependent plasticity at neocortical synapses. We therefore compared properties of neocortical LTD and LTP at layer 2/3 synapses in visual cortex of WT and Ube3a^{m-/p+} mice at both young (~P25) and adult (~P100) ages. Because layer 2/3 pyramidal neurons receive major inputs from layer 4 pyramidal neurons, layer 2/3 field potentials were evoked by layer 4 stimulation (Fig. 3a). We began by measuring LTD in young mice using a standard stimulation protocol (1 Hz for 15 min). Whereas LTD was reliably induced in young WT mice, it was absent in young Ube3a^{m-/p+} mice (Fig. 3b). We also observed deficits in LTP induction. While a relatively weak induction protocol (three 1 second trains of 40 Hz stimulation) elicited LTP in young WT mice, this protocol failed to reliably induce LTP in young Ube3a^{m-/p+} mice (Fig. 3c). To test whether the neocortex of Ube3a^{m-/p+} mice was capable of expressing LTP, we also applied a strong LTP stimulation protocol (two 1 sec trains of 100 Hz stimulation). This protocol consistently induced LTP in both Ube3a^{m-/p+} and WT mice (Fig. 3d). Thus, as with LTP deficits in hippocampus^{8,9}, LTP

induction machinery is impaired in the visual cortex of *Ube3a^{m-/p+}* mice and this deficit in LTP can be overcome with strong stimulation. Unexpectedly, the impairment in plasticity is bidirectional, as *Ube3a* was also required for the normal induction of both LTD and LTP (Fig. 3e), indicating profound synaptic rigidity.

To determine whether the plasticity deficits in AS mice persisted into adulthood, we tested LTP and LTD at adult (~P100) ages. In adult WT mice, LTD induced by 1 Hz stimulation was absent as expected²⁷, and LTP could be induced with strong stimulation (two trains of 100 Hz stimulations) (Supplementary Fig. 3b, c, d). In adult *Ube3a^{m-/p+}* mice, however, none of these protocols were effective at modifying synaptic strength (Supplementary Fig. 3b, c, d). These results indicate that WT animals exhibit attenuated neocortical plasticity as they mature, and this attenuation of plasticity is even more severe in the absence of *Ube3a* (compare Fig. 3e and Supplementary Fig. 3e). Further, these data show that plasticity defects in AS mice persist into adulthood.

Sensory experience dampens cortical plasticity in AS mice

Visual experience can alter the ability to induce LTD and LTP^{20,28}. Therefore, we speculated that the LTD and LTP impairments in *Ube3a^{m-/p+}* mice could result from an inappropriately strong downregulation of synaptic plasticity induced by visual experience. In this case, one would expect that animals with no previous visual experience would possess normal synaptic plasticity. We investigated this possibility by measuring LTD and LTP in young WT and *Ube3a^{m-/p+}* mice reared in the dark (Fig. 4a, b). Indeed, visual deprivation in *Ube3a^{m-/p+}* mice restored the normal induction and expression of LTP (induced by the 40 Hz protocol) and LTD (induced by a 1 Hz protocol) (Fig. 4c,d). Thus, sensory deprivation prevents synaptic plasticity impairments in *Ube3a^{m-/p+}* mice. In other words, *Ube3a^{m-/p+}* mice are born with normal LTD and LTP at neocortical synapses, but ongoing sensory experiences impair the induction/expression of synaptic plasticity in the absence of *Ube3a*.

To test if the experience-dependent loss of synaptic plasticity observed by field potential recordings is due to the loss of plasticity at excitatory synapses on layer 2/3 pyramidal neurons, we conducted voltage-clamp recordings of excitatory currents in layer 2/3 neurons (Supplementary Fig. 4). Consistent with the field potential recordings, 1 Hz stimulation paired with postsynaptic depolarization induced LTD in NR young (P25) WT mice, but the same protocol failed to reliably induce LTD in NR *Ube3a^{m-/p+}* mice (Supplementary Fig. 4d, f). Moreover, dark-rearing partially recovered LTD in *Ube3a^{m-/p+}* mice to levels comparable to dark-reared WT mice (Supplementary Fig. 4d, f). These data provide further evidence that sensory-driven activity attenuates synaptic plasticity in the absence of *Ube3a*. In support of this idea, LTD was induced normally in layer 2/3 pyramidal neurons of *Ube3a^{m-/p+}* mice at P10, before eye opening (Supplementary Fig. 4c, f).

To verify that visual experience, rather than an intrinsic developmental program, caused the loss of plasticity in *Ube3a^{m-/p+}* mice, we investigated the effect of reinstating sensory experience following dark rearing. To this end, we dark-reared mice until ~P25, and then provided them with one or four days of a normal visual environment (Fig. 4e). Although LTD was readily induced in the layer 4 to 2/3 pathway of visual cortex in WT mice after one day of visual experience, LTD appeared reduced in *Ube3a^{m-/p+}* mice (Fig. 4f, h). After four days of visual experience, LTD was completely abolished in *Ube3a^{m-/p+}* mice (Fig. 4g, h), indicating that relatively brief (<4 days) visual experience was sufficient to cause a loss of normal plasticity in AS animals.

Late-onset deprivation recovers plasticity in AS mice

Can sensory deprivation recover plasticity in normally reared $Ube3a^{m-/p+}$ mice at later stages, after the ability to induce plasticity has already been driven down by previous sensory experience? To answer this question, we reared WT and $Ube3a^{m-/p+}$ mice normally until ~P30 (Fig. 5b), as LTD is absent in AS mice by four weeks of age (Fig. 3b), and then measured plasticity (Fig. 5a) after the mice had been given a late-onset visual deprivation (LOVD) for 10 days (WT = 10 slices, $Ube3a^{m-/p+}$ = 11 slices). As an additional control, LTD was also measured in age-matched WT mice that had been reared normally until ~P40.

We found that 1 Hz LTD was reduced at ~P40 in NR WT mice (Fig. 5c d), similar to previous observations showing a developmental reduction at the field potential level in visual cortex LTD in WT animals^{27,29}. Consistent with a recent finding that LOVD restores synaptic plasticity in adult animals *in vivo*³⁰, LOVD reinstated 1 Hz LTD in WT mice (Fig. 5c, d). Moreover, a similar level of LTD was restored after LOVD in $Ube3a^{m-/p+}$ mice (Fig. 5c, d), suggesting that LOVD recovers LTD even in the absence of Ube3a (Fig. 5d). The LOVD-induced recovery of LTD was also observed in whole-cell recordings from identified layer 2/3 pyramidal neurons (Supplementary Fig. 4e, f). Together, these data demonstrate that LOVD can restore synaptic plasticity in $Ube3a^{m-/p+}$ mice.

Ocular dominance plasticity is absent in AS mice

The severe plasticity deficits recorded in *ex vivo* brain slices suggested that experience-dependent modifications *in vivo* might also be impaired by the absence of Ube3a. We first assessed visual function by recording visual evoked potentials (VEPs) in visual cortex. These measurements revealed that both visual acuity (Supplementary Fig. 5; Supplementary Methods) and baseline ocularity were normal (Fig. 6b, c), suggesting that $Ube3a^{m-/p+}$ mice have grossly normal visual functions.

Next, we investigated *in vivo* plasticity of visual cortical circuits by challenging the mice with monocular deprivation (MD). This sensory manipulation produces a well-characterized ocular dominance shift in wild-type animals and has served as a gauge of critical period plasticity³¹. In the visual cortex, an ocular dominance shift can be observed most prominently during a critical period, which peaks in the third to fourth postnatal week in mice³². At these ages, however, both LTD and LTP were impaired in normally reared $Ube3a^{m-/p+}$ mice (Fig. 3). In WT mice experiencing normal binocular vision, no dramatic change in ocularity from P27-P30 was observed as expected (Fig. 6b). Three days of MD beginning from P27, however, reduced the contralateral bias of WT mice (Fig. 6b), an effect which is particularly robust when comparisons are made between MD mice and their age-matched, non-deprived controls (t-test between monocularly deprived WT mice and age-matched control WT mice, $p < 0.005$). In these experiments eye occlusion is always contralateral to the recording electrode. These data indicate that WT mice are highly susceptible to altered sensory experience at this age.

$Ube3a^{m-/p+}$ mice experiencing binocular vision had similar ocularity on P27 and P30 (Fig 6c). Unlike WT mice, the Ube3a-deficient mice showed no response to three days of MD (Fig. 6c). The ocularity change observed in WT mice was largely due to MD-induced depression of the contralateral VEP response (Fig. 6d). No change in the contralateral response was observed in $Ube3a^{m-/p+}$ mice (Fig. 6e). These results suggest that the experience-dependent loss of synaptic plasticity that occurs in the absence of Ube3a likewise limits the ability to rearrange cortical circuits during the critical period *in vivo*.

Discussion

We have identified a critical role for the AS- and autism-linked ubiquitin ligase Ube3a in experience-dependent neocortical development. We have found that visual experience fails to strengthen functional connectivity of excitatory neurons in the visual cortex of Ube3a^{m-/p+} mice. The lack of experience-dependent development of excitatory circuits is likely caused by deficits in synaptic plasticity, because both LTP and LTD are severely attenuated in Ube3a^{m-/p+} mice. Paradoxically, the plasticity deficit is itself driven by sensory experiences, as sensory deprivation prevents the loss of normal synaptic plasticity, while brief sensory experiences can reinstate the plasticity deficit. Therefore, Ube3a is necessary to maintain normal synaptic plasticity during ongoing activity-dependent remodeling. Finally, we have shown that Ube3a^{m-/p+} mice lack the cortical plasticity that is normally induced by monocular deprivation *in vivo*, demonstrating a role for Ube3a in naturally occurring experience-dependent modifications of neuronal circuits. The neocortical plasticity deficits caused by the absence of Ube3a may thus underlie the learning deficits observed in Angelman syndrome.

Two possibilities could explain the plasticity deficits in Ube3a^{m-/p+} mice. First, cooperative excitatory drive may be attenuated in Ube3a-deficient mice, thus increasing the induction parameters for LTD and LTP. This could arise from a decrease in the number of excitatory synapses or their release probability, both of which are consistent with the observed reduction in spine density and mEPSC frequency of layer 2/3 pyramidal neurons. The possibility that Ube3a^{m-/p+} mice exhibit abnormal neurotransmitter release might be particularly relevant for the LTD deficit in layers 2/3, as recent evidence suggests that LTD induced at this synapse requires endocannabinoid-mediated reductions in presynaptic neurotransmitter release³³. Future studies are needed to determine whether presynaptic plasticity and/or release mechanisms are disrupted by the absence of Ube3a, and whether this might contribute to the observed plasticity deficits.

Alternatively, the machinery for plasticity induction or expression may itself be compromised in Ube3a-deficient mice, including changes in calcium entry, receptor trafficking, or pre/postsynaptic signaling molecules. Indeed, the absence of Ube3a impairs the function of calcium/calmodulin-dependent protein kinase II (CaMKII)⁸, an enzyme which normally facilitates LTP induction³⁴ both in the hippocampus³⁵ and in the visual cortex^{27,36}. Thus, although not yet examined in the neocortex, reductions in CaMKII activity in Ube3a^{m-/p+} mice might contribute to the observed deficits in neocortical LTP. Intriguingly, the cortical LTP deficit observed in CaMKII knockout mice becomes progressively more severe with development²⁷, raising the possibility that the age-dependent increase in the LTP deficits observed in Ube3a-deficient mice may be a consequence of an increasing requirement of CaMKII for LTP induction³⁷. Like LTP, impairments in LTD could also arise from changes in signaling molecules. One such candidate molecule is PP1, as its enzymatic activity is implicated in LTD induction^{38,39} and is attenuated in Ube3a^{m-/p+} mice⁸. If the plasticity induction mechanisms for LTD and LTP are indeed compromised in the neocortex in the absence of Ube3a, then this could feasibly contribute to the observed reductions in spine density.

The ubiquitin-proteasome system is necessary for both LTP⁴⁰ and LTD⁴¹, and our data demonstrate that Ube3a is one critical component of this system. However, the protein substrate (s) of Ube3a, whose degradation is required to maintain normal synaptic plasticity, remain unknown. Extensive GeneChip analyses of the murine visual cortex have revealed that visual experience affects the expression of many genes^{42,43}. If one of these visual experience-induced proteins is a substrate for Ube3a, this protein could be abnormally overexpressed in Ube3a^{m-/p+} mice given visual experience. Furthermore, if the protein has an ability to suppress synaptic plasticity, experience-dependent accumulation of such a protein would attenuate LTD

and LTP in the absence of Ube3a. An ideal substrate of Ube3a that could account directly for the experience-induced plasticity deficits, would thus be a protein that is upregulated by activity but, at high levels, suppresses subsequent synaptic remodeling.

We suggest that the plasticity deficits observed *in vitro* may contribute to or underlie synaptic learning deficits associated with AS. In support of the idea that Ube3a is required for naturally occurring plasticity during a critical period of development, we have found that ocular dominance plasticity is absent in Ube3a^{m-/p+} mice (Fig. 6). Because LTD and monocular deprivation-induced depression of the deprived eye response share a common pathway⁴⁴, visual experience-induced loss of LTD could be the direct cause of the lack of ocular dominance plasticity. Consistent with this idea, Ube3a-deficient mice lacked the loss of responsiveness from the deprived eye that is normally observed following brief monocular deprivation.

Functional^{45,46} and anatomical⁴⁷ abnormalities in the visual system of human AS patients are consistent with the observed aberrant development of visual cortical circuits in Ube3a^{m-/p+} mice. If the deficits in experience-dependent encoding in the visual cortex are generalizable to other areas of the brain, then these same changes in synaptic physiology may explain the observed deficiencies in learning and cognition in human AS patients. It is notable that LOVD restores plasticity in Ube3a^{m-/p+} mice (Fig. 5 and Supplementary Fig. 4e, f). The demonstration that the physiological substrates of synaptic plasticity remain intact raises the possibility that behavioral or pharmacological manipulations could improve brain function in patients with AS. Moreover, because it has been speculated that sensory experience-dependent brain development is abnormal in other neurodevelopmental disorders such as Rett syndrome, Fragile X syndrome, and autism⁷, our experimental approach may help to elucidate roles of experience in these disorders.

Methods

Animals

Mice deficient in Ube3a, originally developed by Jiang et. al.², were obtained through the Jackson Laboratory. Mice were bred on a 129S7 background. To obtain heterozygous mice lacking Ube3a gene paternally (m+/p-) or maternally (m-/p+), a heterozygous male or female mouse was crossed with a wild-type female or male mouse, respectively. For most electrophysiological recordings in slices, WT and maternal heterozygous mice were used at three age groups: infant (P8-11; ~P10), young (P21-28; ~P25), and adult (P94-121; ~P100). For LOVD experiments, WT and maternal heterozygous mice at ~P40 (P37-40) were used. Control mice were raised on a 12 h light/dark cycle, whereas DR mice were raised in complete darkness from P9-P11 (before eye opening) until ~P25. Light exposure was achieved by transferring DR mice into the control condition at P21-P28 and providing 1-4 days in the normal light/dark cycle. LOVD was achieved by transferring NR mice at ~P30 into complete darkness for 10 days. Electrophysiological recordings were obtained from at least three mice for each condition. For *in vivo* electrophysiological recordings, mice were used at ages indicated below. All animal procedures were performed in compliance with the U. S. Department of Health and Human Services and the animal care guidelines at the University of North Carolina and Duke University.

Immunoblot analysis

Tissue lysates were prepared in lysis buffer containing (in mM): 50 Tris, 150 NaCl, 50 NaF, 2 EDTA, 2 EGTA, 1% (v/v) Triton, pH 7.4, and a cocktail of protease and phosphatase inhibitors. Protein concentrations were determined using DC Protein Assay (BioRad). 20 µg of each lysate was resolved on a 7.5% Tris-HCl gel (BioRad), and transferred to a PVDF membrane. The membrane was probed with anti-Ube3a primary antibody (1:1000, Bethyl

Labs) and subsequently with horseradish peroxidase-conjugated anti-rabbit polyclonal antibody (1:10,000, Cell Signaling). Signals were visualized with ECL Plus reagent (Amersham) and an LAS-3000 Intelligent Dark Box (FujiFilm).

Immunohistochemistry

Mice were anesthetized with pentobarbital and perfused intracardially with cold phosphate-buffered saline (PBS) followed by freshly prepared 4% paraformaldehyde in 0.1 M phosphate buffer (pH 7.4). Brains were postfixed in the same solution overnight at 4°C. Brains were then cut into 50 µm coronal sections using a vibratome (Leica Microsystems, Inc.). For immunohistochemistry experiments, sections from wild-type, Ube3a^{m-/p+}, and Ube3a^{m-/p-} mice were always processed simultaneously. Sections were incubated in 10 mM sodium citrate buffer (pH 8.65) at 80°C for 15 min prior to the immunoreactions. Sections were reacted with anti-Ube3a rabbit polyclonal antibody (1:500, Bethyl Labs) and anti-NeuN monoclonal mouse antibody (1:3000, Chemicon) overnight at 4°C, and were then incubated with Alexa Fluor 488 goat anti-mouse IgG and Alexa Fluor 568 goat anti-rabbit IgG secondary antibodies (1:500, Invitrogen). Images were acquired using a Zeiss LSM 510 laser scanning confocal microscope.

Visual cortical slice preparation

Mice were anesthetized with an overdose of pentobarbital and decapitated after the disappearance of corneal reflexes. Brains were dissected rapidly and the visual cortex cut coronally at 300 µm (voltage-clamp recordings) or 400 µm (field potential recordings) in dissection buffer containing the following (in mM): 75 sucrose, 87 NaCl, 2.5 KCl, 1.25 NaH₂PO₄, 26 NaHCO₃, 10 glucose, 7 MgCl₂, 0.5 CaCl₂, and 1.3 ascorbic acid. Prior to recordings, slices were allowed to recover for one hour in a submersion chamber containing oxygenated artificial cerebrospinal fluid (ACSF) consisting of the following (in mM): 124 NaCl, 3 KCl, 1.25 NaH₂PO₄, 26 NaHCO₃, 20 glucose, 2 MgCl₂, and 1 CaCl₂. For patch clamp recordings, slices were allowed to recover in a submersion chamber, which was preheated to 35°C and gradually cooled to room temperature. For field recordings, slices were allowed to recover in a submersion chamber, which was precooled to 5–10 °C and gradually warmed to room temperature.

Voltage-clamp recordings

mEPSC recordings—Slices were placed in a submersion chamber, maintained at 30°C, and perfused at 2 ml/min with oxygenated ACSF supplemented with 200 nM tetrodotoxin, 100 µM APV, and 50 µM picrotoxin. Neurons were visualized with a Carl Zeiss Axioskop equipped with infrared differential interference contrast optics. Patch pipettes were pulled from thick-walled borosilicate glass. Open tip resistances were 3–5 MΩ when pipettes were filled with the internal solution containing (in mM): 20 KCl, 100 (K)Gluconate, 10 (K)HEPES, 4 (Mg) ATP, 0.3 (Na)GTP, 10 (Na)Phosphocreatine, and 0.01% w/v Alexa 488, adjusted with KOH to pH 7.4, and with sucrose to 290–300 mOsm. Voltage-clamp recordings were performed in the whole-cell configuration with a patch-clamp amplifier (Multiclamp 700A, Molecular Devices), and data were acquired with pClamp 9.2 software (Molecular Devices). Input and series resistances were determined throughout the experiment by measuring the response to small intermittent test pulses. Recordings were discarded if the series resistance grew larger than 25 MΩ, or the resting potential was more positive than -60 mV (for the recordings in infant mice, the resting potential was not used as a criterion, as many neurons typically exhibit resting potentials higher than -60 mV). Analysis was restricted to neurons that were anatomically verified by intracellular fills to be pyramidal neurons. MiniAnalysis (Synaptosoft) was used to detect and measure mEPSCs. The threshold to detect mEPSC was set at 5 pA, which is greater than 2.5 times the root mean square of the noise, and mEPSCs

with 10–90% rise times more than 3 ms were excluded from the analysis. Analysis of mEPSCs was performed blind to age, genotype, and rearing condition.

Field potential recordings

Slices were maintained at 30°C and perfused with ACSF at a rate of 2 ml/min. A concentric bipolar tungsten stimulation electrode was positioned in layer 4, and a glass recording electrode (1–3 MΩ) filled with ACSF was positioned in layers 2/3. The magnitude of responses evoked by a 200 μs pulse was monitored by the amplitude of the field potential. Stimulation intensity was adjusted to elicit half the maximal response, and stable baseline responses were elicited every 30 s. The resulting signals were filtered between 0.1 Hz and 3 kHz, amplified, and captured at 10 kHz using pCLAMP 9.2 software (Molecular Devices). After achieving a stable baseline (<5% drift) for 15 min, slices were stimulated with one of the following three protocols: 100 Hz stimulation for 1 s, repeated two times with a 15 s interval; 40 Hz stimulation for 1 s, repeated three times with 10 s intervals; or 900 pulses at 1 Hz. Field excitatory postsynaptic potential (fEPSP) amplitudes were recorded every 30 s for 45 min following cessation of the stimulation protocol. Control and experimental subjects were run in an interleaved fashion. Normalized averaged data were reported as means ± SEM. Changes in synaptic strength were measured by comparing the average response amplitudes 30–45 min after conditioning stimulation to the pre-conditioning baseline response.

Morphological analysis by Golgi staining

Littermates at P25–26 reared in a normal environment (NR WT, n = 4 mice; NR Ube3a^{m-/p+}, n = 3 mice) or in complete darkness from P10 (DR WT, n = 3 mice; DR Ube3a^{m-/p+}, n = 4 mice) were used. Mice were anesthetized with pentobarbital and perfused intracardially with cold phosphate-buffered saline (PBS) followed by freshly prepared 4% paraformaldehyde in 0.1 M phosphate buffer (pH 7.4). After post-fixation in the same solution, tissue blocks containing visual cortex were processed according to a modification of the Golgi-Kopsch technique⁴⁸. 100 μm-thick serial sections were collected for study. Pyramidal neurons at layer 2/3 of the visual cortex were chosen and spines in 13 μm dendritic segments taken 30–50 μm from the soma were counted under a 100× oil immersion lens. Analyses were performed blind to genotype. Images were taken on a Leica TCS SP2 laser scanning confocal microscope using the 488 nm laser line as a light source. To obtain high-resolution images of impregnated dendrites, stacks were taken with a 100× objective at 0.3663 μm intervals at 4× zoom. Dendritic segments were cropped from the resulting stacks and processed by 3D-deconvolution using the AutoQuant software (Media Cybernetics).

Visual evoked potential recordings

Male and female mice were anesthetized with ketamine/xylazine 120/9 mg/kg i.p. (Southern Anesthesia) and locally at the scalp incision site with 0.25% bupivacaine (Hospira). Tungsten microelectrodes (FHC) with tip impedances of 0.3–0.5 MΩ were stereotaxically implanted in the binocular zone of the visual cortex: lambda 0.0 mm (anterior/posterior), sagittal ±3.00 mm (medial/lateral), and depth -0.45 mm (dorsal/ventral). Silver reference electrodes were implanted -1.0 mm anterior/posterior to bregma, ±2.00 mm sagittal, at a depth just touching the brain surface. Electrodes were secured to the skull with Loctite 455 cyanoacrylate (Henkel).

Electrodes were implanted at P22–23 and animals were habituated 24 h prior to the first recording session at P27–28. Visual stimuli consisted of full-field diagonal (135° or 45°, reversed on day 3) sine wave gratings at 0.3 cpd and 100% contrast. Visual potentials were evoked monocularly through the eye ipsilateral and contralateral to the recording electrode. Following baseline ocularity VEP recordings, one eye was sutured closed. Mice were anesthetized with 1.5% isoflurane, lid margins were trimmed, and three stitches were applied along the length of the lids using 5-0 silk. Mice were monocularly deprived in the eye

contralateral to the recording electrode for three days. The stitched eye was then reopened and visual potentials were again evoked monocularly through the eye ipsilateral and contralateral to the recording electrode to measure the ocular dominance shift. To quantify ocular dominance plasticity, measurements were made as a ratio of the contralateral (deprived) to ipsilateral (non-deprived) eye responses (Fig. 6b,c) or as raw amplitudes (Fig. 6d,e). As a control for developmental changes, VEP recordings were performed in mice which did not receive monocular deprivation.

Statistics

Data are expressed as the means \pm SEM. Unless noted, unpaired two-tailed Student's *t* tests were used to test for statistical significance, which was placed at $p < 0.05$. Raw values for the data shown in Figures 1-6 can be found in Supplementary Table 2.

Supplementary Material

Refer to Web version on PubMed Central for supplementary material.

Acknowledgments

We thank Ian Davison, Serena Dudek, Paul Farel, Paul Manis, Richard Mooney, Robert Sealock, Mark Zylka, and members of the Philpot and Ehlers labs for critical readings of the manuscript and helpful discussions. We also thank Rylan Larsen, Peter Cao of the UNC Summer Undergraduate Research Experience Program, Robert Peterson at the UNC Confocal/Multiphoton Microscopy Core Facility, and Kirk McNaughton at the UNC Histology Facility for technical help. Special thanks to William Boyes, Jacqueline deMarchena, Lena Khibnik, Rahmat Muhammad, and Mark Bear for their assistance with the VEP technique. This work was supported by a UNC dissertation completion fellowship (K.Y.), Ruth K. Broad Biomedical Research Foundation Inc. Graduate Student Research Award (K.H.C.), Helen Lyng White Fellowship and a NICHD training grant T32-HD40127 (A.C.R.), NIH grants NS039402 and AG024492 (M.D.E.), NINDS NS035527 (R.J.W.), NEI R01EY018323 (B.D.P.), and the Angelman Syndrome Foundation and Simons Foundation (B.D.P. and M.D.E.). M.D.E. is an Investigator of the Howard Hughes Medical Institute.

References

1. Clayton-Smith J, Laan L. Angelman syndrome: a review of the clinical and genetic aspects. *J Med Genet* 2003;40:87–95. [PubMed: 12566516]
2. Jiang YH, et al. Mutation of the Angelman ubiquitin ligase in mice causes increased cytoplasmic p53 and deficits of contextual learning and long-term potentiation. *Neuron* 1998;21:799–811. [PubMed: 9808466]
3. Rougeulle C, Glatt H, Lalonde M. The Angelman syndrome candidate gene, UBE3A/E6-AP, is imprinted in brain. *Nat Genet* 1997;17:14–5. [PubMed: 9288088]
4. Schroer RJ, et al. Autism and maternally derived aberrations of chromosome 15q. *Am J Med Genet* 1998;76:327–36. [PubMed: 9545097]
5. Albrecht U, et al. Imprinted expression of the murine Angelman syndrome gene, Ube3a, in hippocampal and Purkinje neurons. *Nat Genet* 1997;17:75–8. [PubMed: 9288101]
6. Dindot SV, Antalffy BA, Bhattacharjee MB, Beaudet AL. The Angelman syndrome ubiquitin ligase localizes to the synapse and nucleus, and maternal deficiency results in abnormal dendritic spine morphology. *Hum Mol Genet*. 2007
7. Zoghbi HY. Postnatal neurodevelopmental disorders: meeting at the synapse? *Science* 2003;302:826–30. [PubMed: 14593168]
8. Weeber EJ, et al. Derangements of hippocampal calcium/calmodulin-dependent protein kinase II in a mouse model for Angelman mental retardation syndrome. *J Neurosci* 2003;23:2634–44. [PubMed: 12684449]
9. van Woerden GM, et al. Rescue of neurological deficits in a mouse model for Angelman syndrome by reduction of alphaCaMKII inhibitory phosphorylation. *Nat Neurosci* 2007;10:280–2. [PubMed: 17259980]

10. Yi JJ, Ehlers MD. Ubiquitin and protein turnover in synapse function. *Neuron* 2005;47:629–32. [PubMed: 16129392]
11. Yi JJ, Ehlers MD. Emerging roles for ubiquitin and protein degradation in neuronal function. *Pharmacol Rev* 2007;59:14–39. [PubMed: 17329546]
12. Walz NC, Baranek GT. Sensory processing patterns in persons with Angelman syndrome. *Am J Occup Ther* 2006;60:472–9. [PubMed: 16915878]
13. Williams CA, et al. Angelman syndrome 2005: updated consensus for diagnostic criteria. *Am J Med Genet A* 2006;140:413–8. [PubMed: 16470747]
14. Hensch TK. Critical period plasticity in local cortical circuits. *Nat Rev Neurosci* 2005;6:877–88. [PubMed: 16261181]
15. Fagiolini M, et al. Separable features of visual cortical plasticity revealed by N-methyl-D-aspartate receptor 2A signaling. *Proc Natl Acad Sci U S A* 2003;100:2854–9. [PubMed: 12591944]
16. Gianfranceschi L, et al. Visual cortex is rescued from the effects of dark rearing by overexpression of BDNF. *Proc Natl Acad Sci U S A* 2003;100:12486–91. [PubMed: 14514885]
17. Li Y, Fitzpatrick D, White LE. The development of direction selectivity in ferret visual cortex requires early visual experience. *Nat Neurosci* 2006;9:676–81. [PubMed: 16604068]
18. Wallace W, Bear MF. A morphological correlate of synaptic scaling in visual cortex. *J Neurosci* 2004;24:6928–38. [PubMed: 15295028]
19. Philpot BD, Sekhar AK, Shouval HZ, Bear MF. Visual experience and deprivation bidirectionally modify the composition and function of NMDA receptors in visual cortex. *Neuron* 2001;29:157–69. [PubMed: 11182088]
20. Kirkwood A, Rioult MG, Bear MF. Experience-dependent modification of synaptic plasticity in visual cortex. *Nature* 1996;381:526–528. [PubMed: 8632826]
21. Jordan C, Francke U. Ube3a expression is not altered in Mecp2 mutant mice. *Hum Mol Genet* 2006;15:2210–5. [PubMed: 16754645]
22. Vu TH, Hoffman AR. Imprinting of the Angelman syndrome gene, UBE3A, is restricted to brain. *Nat Genet* 1997;17:12–3. [PubMed: 9288087]
23. Mullen RJ, Buck CR, Smith AM. NeuN, a neuronal specific nuclear protein in vertebrates. *Development* 1992;116:201–11. [PubMed: 1483388]
24. Desai NS, Cudmore RH, Nelson SB, Turrigiano GG. Critical periods for experience-dependent synaptic scaling in visual cortex. *Nat Neurosci* 2002;5:783–9. [PubMed: 12080341]
25. Goel A, Lee HK. Persistence of experience-induced homeostatic synaptic plasticity through adulthood in superficial layers of mouse visual cortex. *J Neurosci* 2007;27:6692–700. [PubMed: 17581956]
26. Nimchinsky EA, Sabatini BL, Svoboda K. Structure and function of dendritic spines. *Annu Rev Physiol* 2002;64:313–53. [PubMed: 11826272]
27. Kirkwood A, Silva A, Bear MF. Age-dependent decrease of synaptic plasticity in the neocortex of α CaMKII mutant mice. *Proc Natl Acad Sci* 1997;94:3380–3383. [PubMed: 9096402]
28. Philpot BD, Cho KK, Bear MF. Obligatory Role of NR2A for Metaplasticity in Visual Cortex. *Neuron* 2007;53:495–502. [PubMed: 17296552]
29. Jiang B, Trevino M, Kirkwood A. Sequential development of long-term potentiation and depression in different layers of the mouse visual cortex. *J Neurosci* 2007;27:9648–52. [PubMed: 17804625]
30. He HY, Hodos W, Quinlan EM. Visual deprivation reactivates rapid ocular dominance plasticity in adult visual cortex. *J Neurosci* 2006;26:2951–5. [PubMed: 16540572]
31. Wiesel TN, Hubel DH. Single cell responses in striate cortex of kittens deprived of vision in one eye. *J Neurophysiol* 1963;26:1003–1017. [PubMed: 14084161]
32. Gordon JA, Stryker MP. Experience-dependent plasticity of binocular responses in the primary visual cortex of the mouse. *J Neurosci* 1996;16:3274–86. [PubMed: 8627365]
33. Crozier RA, Wang Y, Liu CH, Bear MF. Deprivation-induced synaptic depression by distinct mechanisms in different layers of mouse visual cortex. *Proc Natl Acad Sci U S A* 2007;104:1383–8. [PubMed: 17227847]
34. Xia Z, Storm DR. The role of calmodulin as a signal integrator for synaptic plasticity. *Nat Rev Neurosci* 2005;6:267–76. [PubMed: 15803158]

35. Silva A, Stevens C, Tonegawa S, Wang Y. Deficient hippocampal long-term potentiation in α -calcium-calmodulin kinase II mutant mice. *Science* 1992;257:206–211. [PubMed: 1321493]
36. Frankland PW, O'Brien C, Ohno M, Kirkwood A, Silva AJ. Alpha-CaMKII-dependent plasticity in the cortex is required for permanent memory. *Nature* 2001;411:309–13. [PubMed: 11357133]
37. Yasuda H, Barth AL, Stellwagen D, Malenka RC. A developmental switch in the signaling cascades for LTP induction. *Nat Neurosci* 2003;6:15–6. [PubMed: 12469130]
38. Torii N, Kamishita T, Otsu Y, Tsumoto T. An inhibitor for calcineurin, FK506, blocks induction of long-term depression in rat visual cortex. *Neurosci Lett* 1995;185:1–4. [PubMed: 7537357]
39. Mulkey RM, Endo S, Shenolikar S, Malenka RC. Involvement of a calcineurin/inhibitor-1 phosphatase cascade in hippocampal long-term depression. *Nature* 1994;369:486–8. [PubMed: 7515479]
40. Fonseca R, Vabulas RM, Hartl FU, Bonhoeffer T, Nagerl UV. A balance of protein synthesis and proteasome-dependent degradation determines the maintenance of LTP. *Neuron* 2006;52:239–45. [PubMed: 17046687]
41. Colledge M, et al. Ubiquitination regulates PSD-95 degradation and AMPA receptor surface expression. *Neuron* 2003;40:595–607. [PubMed: 14642282]
42. Majdan M, Shatz CJ. Effects of visual experience on activity-dependent gene regulation in cortex. *Nat Neurosci*. 2006
43. Tropea D, et al. Gene expression changes and molecular pathways mediating activity-dependent plasticity in visual cortex. *Nat Neurosci* 2006;9:660–8. [PubMed: 16633343]
44. Heynen AJ, et al. Molecular mechanism for loss of visual cortical responsiveness following brief monocular deprivation. *Nat Neurosci* 2003;6:854–62. [PubMed: 12886226]
45. Van Splunder J, Stilma JS, Evenhuis HM. Visual performance in specific syndromes associated with intellectual disability. *Eur J Ophthalmol* 2003;13:566–74. [PubMed: 12948316]
46. Thompson DA, Kriss A, Cottrell S, Taylor D. Visual evoked potential evidence of albino-like chiasmal misrouting in a patient with Angelman syndrome with no ocular features of albinism. *Dev Med Child Neurol* 1999;41:633–8. [PubMed: 10503922]
47. Jay V, Becker LE, Chan FW, Perry TL Sr. Puppet-like syndrome of Angelman: a pathologic and neurochemical study. *Neurology* 1991;41:416–22. [PubMed: 2006012]
48. Gatenby, J.; Beams, H. *Microscopist's Vade-Mecum*. Vol. 11th. 1950.

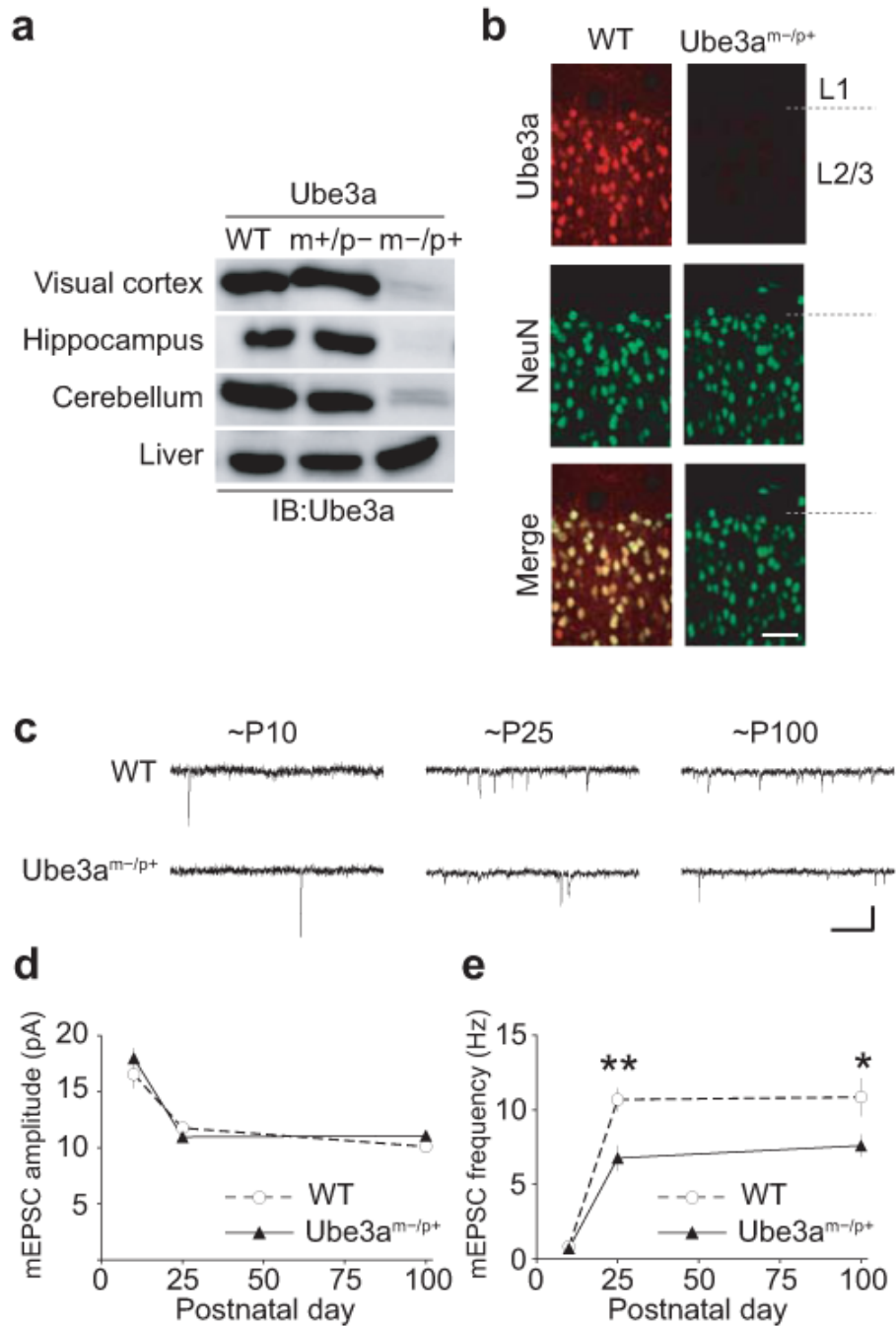


Figure 1. Reduced functional maturation of neocortical synapses in AS mice

a, Immunoblot (IB) analysis of Ube3a in tissue from young (P26) WT, Ube3a^{m+/p-}, and Ube3a^{m-/p+} mice. **b**, Immunohistochemical analysis of Ube3a expression in the visual cortex from young (P24) WT and Ube3a^{m-/p+} mice. Strong Ube3a immunoreactivity was observed in layer 2/3 (L2/3) neurons of WT mice. NeuN antibody stains cell bodies of neurons. Scale bars, 50 μ m. **c**, Representative traces of mEPSCs recorded in L2/3 pyramidal neurons from WT (upper) or Ube3a^{m-/p+} (lower) mice at ~P10, ~P25, and ~P100. Scale bars, 0.2 sec, 20 pA. **d**, Average mEPSC amplitude as a function of postnatal age in WT (P10, n = 11 cells; P25, n = 11 cells; P100, n = 12 cells) and Ube3a^{m-/p+} mice (P10, n = 11 cells; P25, n = 12 cells; P100, n = 12 cells).

n =12 cells). **e**, Average mEPSC frequency as a function of postnatal age in WT and *Ube3a^{m-/p+}*. * $p < 0.05$, ** $p < 0.005$. Error bars in this and all subsequent figures represent s.e.m.

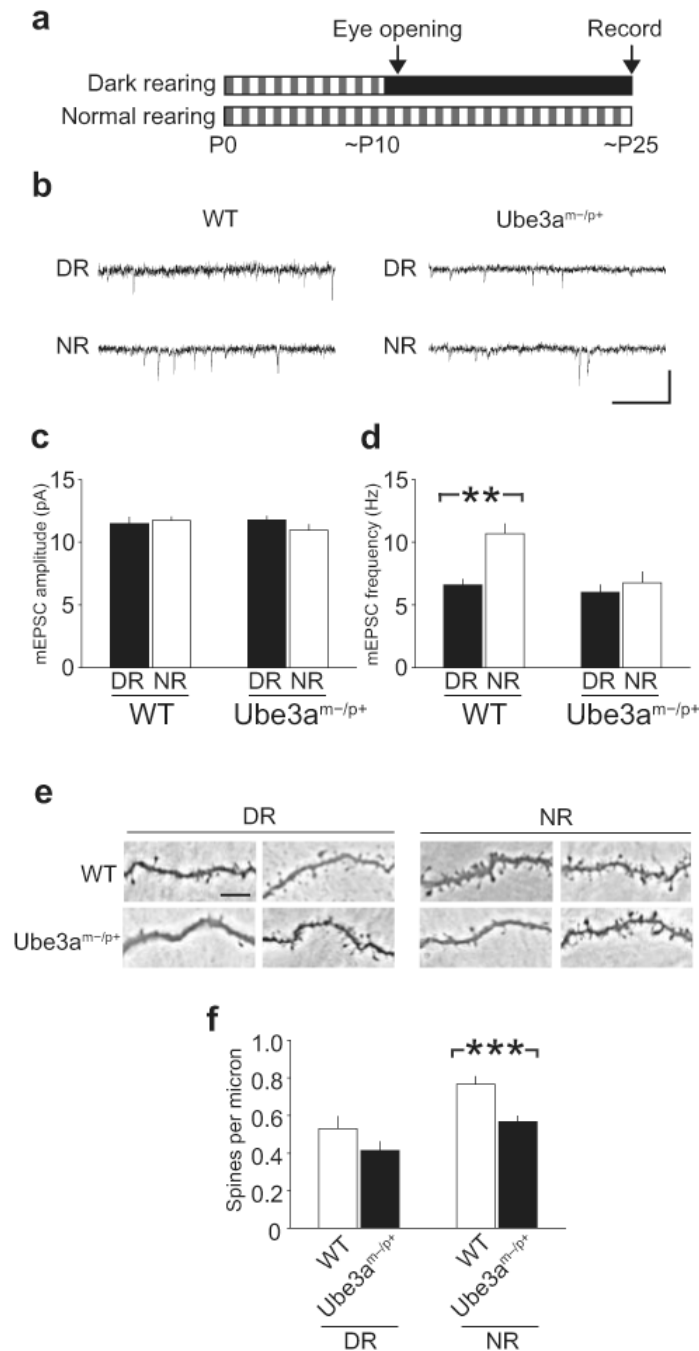


Figure 2. Sensory experience augments excitatory synaptic connections in the neocortex of WT mice, but not AS mice

a, Schematic for the rearing conditions. Normally-reared (NR) animals were maintained in a 12 h consecutive dark:light cycle, and dark-reared (DR) animals were kept in complete darkness from ~P10. **b**, Representative traces of mEPSCs recorded in layer 2/3 pyramidal neurons in young WT (left) or *Ube3a^{m-/p+}* (right) mice reared in complete darkness (DR) or normally (NR). Scale bar: 0.2 sec, 20 pA. **c**, Dark-rearing does not affect mEPSC amplitude in WT (DR, n = 12 cells; NR, n = 11 cells) or *Ube3a^{m-/p+}* mice (DR, n = 14 cells; NR, n = 12 cells). **d**, Dark-rearing significantly reduces mEPSC frequency in WT mice, but does not affect mEPSC frequency in *Ube3a^{m-/p+}* mice. **e**, Representative images of basal dendrites of layer

2/3 pyramidal neurons visualized with Golgi staining. Scale bar, 10 μm . **f**, Average density of dendritic spines in DR (WT, n = 25 cells; Ube3a^{m-/p+}, n = 25 cells) and in NR (WT, n = 33 cells; Ube3a^{m-/p+}, n = 32 cells). *** p < 0.0005.

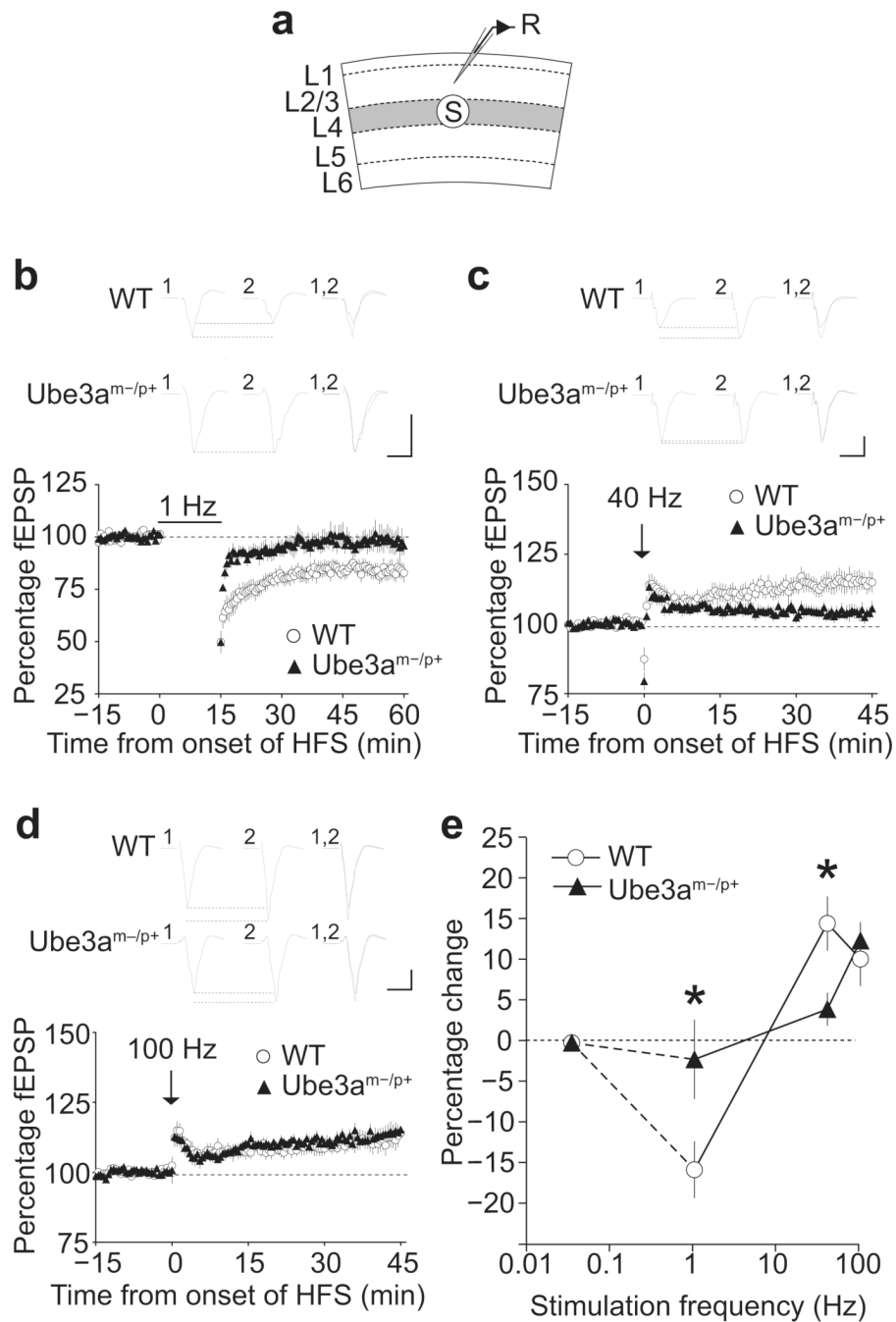


Figure 3. Synaptic plasticity is impaired bidirectionally in the neocortex of AS mice

a, Schematic diagram of stimulating (S) and recording (R) configuration. **b**, Baseline synaptic responses of WT (open circle) and Ube3a^{m-/p+} (closed triangle) mice were measured before and after application of conditioning stimuli to the layer 4 (L4) to L2/3 pathway of the visual cortex. Top traces are representative averaged traces of 15 min baseline (1), 30-45 min period after LTD induction (2), and their overlays (1, 2). Scale bars: 10 ms, 1 mV. The bottom graph describes average change in field EPSP (% fEPSP) upon delivery of a 1 Hz stimulus (indicated by the bar). Whereas 1 Hz stimulation for 15 min induced LTD in young WT mice, it did not change fEPSP amplitudes in Ube3a^{m-/p+} mice (Percentage field excitatory postsynaptic potential (fEPSP): WT, n = 13 slices; Ube3a^{m-/p+}, n = 7 slices; p < 0.04). **c**, Same as **b**, except

that a stimulus consisting of three 40 Hz trains was delivered (indicated by an arrow). While this stimulation induced LTP in WT mice, it did not alter fEPSP amplitudes in Ube3a^{m-/p+} mice (WT, n = 12 slices; Ube3a^{m-/p+}, n = 10 slices; p < 0.02). **d**, Same as c, except that the stimulus consisted of two 100 Hz trains (indicated by an arrow). This stimulation induced LTP in both genotypes (WT, n = 12 slices; Ube3a^{m-/p+}, n = 10 slices; p = 0.59). **e**, Frequency-response functions derived from visual cortex of WT and Ube3a^{m-/p+} mice. Data points represent percent changes in fEPSP 30-45 min after the delivery of conditioning stimuli. The data points for 0.033 Hz are inferred from baseline stimulation delivered once every 30 sec, which induced no obvious synaptic modifications.

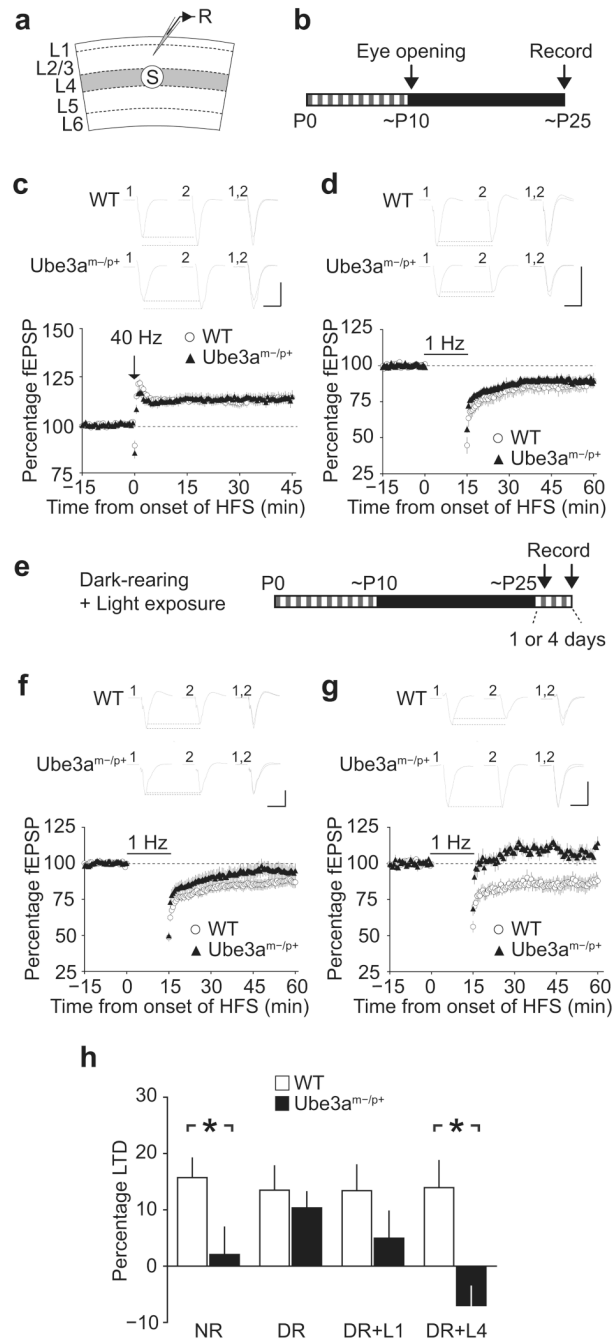


Figure 4. Sensory experience eliminates neocortical plasticity in AS mice

a, Schematic of the recording configuration. **b**, Schematic for the dark-rearing condition. **c**, Representative waveforms and averaged data demonstrating that the level of LTP induced with 40 Hz stimulation is comparable between WT ($n = 18$) and Ube3a^{m-/p+} ($n = 18$) mice reared in complete darkness ($p = 0.91$). Scale bars: 10 ms, 0.5 mV. **d**, The level of LTD is also comparable between WT and Ube3a^{m-/p+} dark-reared mice (WT, $n = 16$ slices; Ube3a^{m-/p+}, $n = 17$ slices; $p = 0.69$). **e**, Schematic showing the schedule for exposing dark-reared mice to light. **f**, One day of normal-rearing following dark-rearing attenuates LTD in visual cortical slices from Ube3a^{m-/p+} mice (WT, $n = 19$; Ube3a^{m-/p+}, $n = 15$; $p = 0.08$). **g**, Four days of normal-rearing following dark-rearing completely suppresses LTD in visual cortical slices

from Ube3a^{m-/p+} mice (WT, n = 9; Ube3a^{m-/p+}, n = 6; p < 0.01). **h**, Visual experience dampens LTD in the visual cortex of Ube3a^{m-/p+} mice. Data represent means ± SEM of the percent reduction in fEPSP 30-45 min after the delivery of conditioning stimuli measured in normally-reared (NR), dark-reared (DR), and dark-then-light exposed for 1 or 4 days (DR+1L, DR+4L) mice.

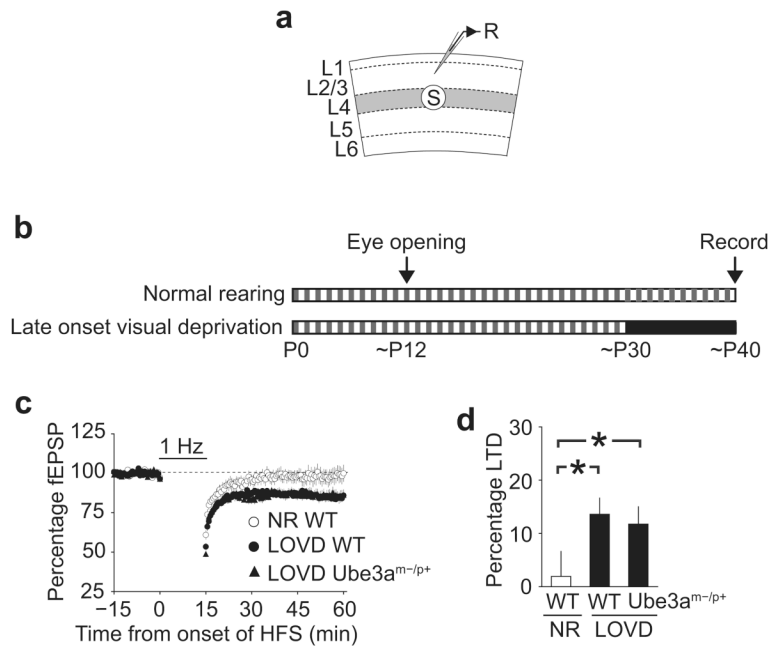


Figure 5. Late-onset visual deprivation restores synaptic plasticity in AS mice

a, Schematic of the recording configuration. **b**, Schematic for the late-onset visual deprivation (LOVD) rearing condition. **c**, Averaged data demonstrating that LTD is abolished in normally reared (NR) WT mice at ~P40, while LTD of a similar magnitude was induced after LOVD in WT and Ube3a^{m-/p+} mice (% fEPSP: NR WT, n = 10 slices; LOVD WT, n = 10 slices; LOVD Ube3a^{m-/p+}, n = 11 slices; p < 0.05, NR WT is significantly different from both LOVD WT and LOVD Ube3a^{m-/p+}, one-way ANOVA followed by Tukey). **d**, Bar graph of data shown in c.

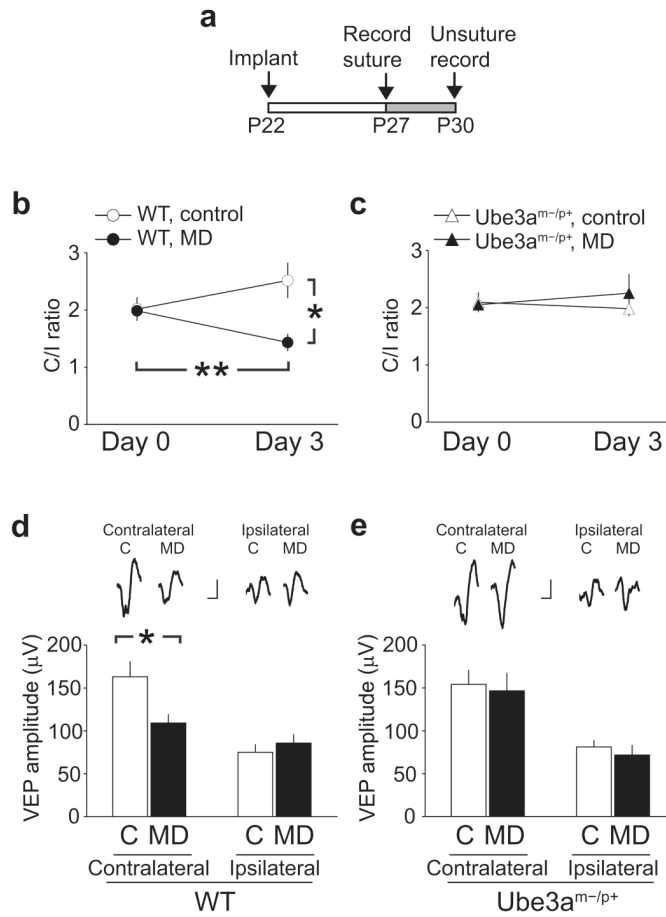


Figure 6. Critical period ocular dominance plasticity is absent in AS mice

a, Schedule of the surgery and recording. **b**, Changes in the ratio of contralateral to ipsilateral eye responses (C/I ratio) in MD (n = 13 mice) and non-deprived control WT mice (n = 14 mice) from P27 (Day 0) to P30 (Day 3). After 3 days of MD, the C/I ratio was significantly reduced (paired t-test $p < 0.01$), whereas this reduction was not observed in age-matched non-deprived controls (paired t-test $p = 0.14$). **c**, C/I ratios in Ube3a^{m-/p+} mice (MD = 11 mice, control = 9 mice). MD did not affect the C/I ratio (paired t-test $p = 0.52$). C/I ratio was stable for 3 days in age-matched non-deprived controls (paired t-test $p = 0.53$). **d**, MD-induced changes in contralateral but not ipsilateral VEPs in WT mice. Top traces are representative waveforms of VEPs recorded in WT mice. Scale bars: 50 μV, 50 msec. The bottom graph describes comparisons of VEP amplitudes between control and monocularly deprived WT mice (* $p < 0.05$). **e**, Same as **d** except that experiments were conducted in Ube3a^{m-/p+} mice.